

## Dimensional crossover in anisotropic Kondo lattices

This article has been downloaded from IOPscience. Please scroll down to see the full text article.

2007 J. Phys.: Condens. Matter 19 406203

(<http://iopscience.iop.org/0953-8984/19/40/406203>)

View [the table of contents for this issue](#), or go to the [journal homepage](#) for more

Download details:

IP Address: 129.252.86.83

The article was downloaded on 29/05/2010 at 06:08

Please note that [terms and conditions apply](#).

## Dimensional crossover in anisotropic Kondo lattices

D Reyes<sup>1</sup> and M A Continentino<sup>2</sup>

<sup>1</sup> Centro Brasileiro de Pesquisas Físicas—Rua Dr Xavier Sigaud, 150-Urca, 22290-180, RJ, Brazil

<sup>2</sup> Instituto de Física, Universidade Federal Fluminense, Campus da Praia Vermelha, Niterói, RJ, 24.210-340, Brazil

E-mail: [daniel@cbpf.br](mailto:daniel@cbpf.br) and [mucio@if.uff.br](mailto:mucio@if.uff.br)

Received 6 July 2007, in final form 15 August 2007

Published 11 September 2007

Online at [stacks.iop.org/JPhysCM/19/406203](http://stacks.iop.org/JPhysCM/19/406203)

### Abstract

Dimensional crossover in the Kondo necklace model is analyzed using the bond-operator method at zero and finite temperatures. Explicit relations describing quasi-two-dimensional properties are obtained by asymptotically solving the resulting equations. The crossover from two dimensions (2d) to three dimensions (3d) is investigated, turning on the electronic hopping ( $t_{\perp}$ ) of conduction electrons between different planes. In order to give continuity to our analysis, both cases of crossover, quasi-three-dimensional (q3d) and quasi-one-dimensional (q1d), are also investigated. The phase diagram as a function of temperature  $T$ ,  $J/t_{\parallel}$  and  $t_{\perp}/t_{\parallel}$ , where  $t_{\parallel}$  is the hopping within the planes, is calculated. Unusual reentrant behavior in the temperature-dependent antiferromagnetic critical line is found close to two dimensions. Near the isotropic three-dimensional quantum critical point the critical line is described by a standard power law with a square root dependence on the distance to the quantum critical point.

(Some figures in this article are in colour only in the electronic version)

### 1. Introduction

Dimensionality plays a central role in strongly correlated electron systems (SCES) [1]. For instance, explanations based on two-dimensional (2d) theories in the neighborhood of a quantum critical point (QCP) [2–7] have been proposed to explain significant unsolved problems in SCES, such as non-Fermi liquid (NFL) behavior and high-temperature superconductivity. But the real materials to which these ideas have been applied are usually rendered three dimensional (3d) by a finite electronic coupling between their component layers; a 2d-QCP has not been experimentally observed in any bulk 3d system, and mechanisms for dimensional reduction have remained the subject of theoretical conjecture [8, 9]. Thus the very notion of dimensionality can be said to acquire an ‘emergent’ nature: although the individual particles move on a three-dimensional lattice, their collective behavior occurs in lower-dimensional space.

Specifically in heavy-fermion (HF) materials, there have already been diverse theories which propose that quasi-two-dimensional (q2d) systems play a central role in the understanding of anomalous behaviors near a magnetic QCP. Several theories were formulated to explain their unusual properties [10–12]. In this context the spin-density wave (SDW) [11, 12] theory as well as the local quantum critical description [13] can account for the logarithmically divergent specific heat coefficients and quasi-linear resistivities only if the spin fluctuations are q2d. The hypothesis that HF materials involve decoupled layers of spins motivates a search for a mechanism that can generate a q2d environment for the spin fluctuations out of a metal that is manifestly three dimensional. One such frequently cited mechanism is geometric anisotropy. Here, the idea is that turning on the hopping between planes  $t_{\perp}$  leads magnetic long-range order (LRO) at finite temperatures. In this paper, we use the Kondo necklace model [14] as a simple Hamiltonian to explore this line of reasoning. The basic aim of our paper is not to examine whether inter-layer coupling is relevant or irrelevant at the QCP but rather to examine whether anisotropy can set up an environment in which the inter-layer coupling is sufficiently weak for us to consider the system to be quasi-two dimensional in all its properties.

The anisotropic Kondo necklace model (AKNM) is given by

$$H = t_{\parallel} \sum_{i, \delta_1} (\tau_i^x \tau_{i+\delta_1}^x + \tau_i^y \tau_{i+\delta_1}^y) + t_{\perp} \sum_{i, \delta_2} (\tau_i^x \tau_{i+\delta_2}^x + \tau_i^y \tau_{i+\delta_2}^y) + J \sum_i \mathbf{S}_i \cdot \boldsymbol{\tau}_i, \quad (1)$$

where  $\tau_i$  and  $\mathbf{S}_i$  are independent sets of spin-1/2 Pauli operators, representing the conduction electron spins and localized spin operators, respectively.  $\delta_1(\delta_2)$  is the difference between lattice vectors of the in-plane (inter-plane) nearest-neighbor sites.  $t_{\parallel}$  is the hopping within the planes and  $t_{\perp}$  that between them. The last term is the magnetic interaction between conduction electrons and localized spins via the coupling  $J$ .

The plan of the paper is the following. In section 2 we set up the bond-operator formalism. In section 3 we describe the antiferromagnetic (AF) ordered state solving the anisotropic Kondo necklace Hamiltonian via the Green's function method; also we show the order parameters at finite temperatures. Section 4 discusses the Néel line in the AKNM. Using the results obtained in the previous section the thermodynamic phase transition and phase diagrams are discussed in section 5 for both cases, the q2d and q3d AKNM. The case  $\xi \gg 1$  that corresponds to  $d = 1$  will be shown only to give continuity to our analysis. Also the reentrance phenomenon, i.e. two successive transitions for certain parameter values, is analyzed. Finally, in section 6 we give the conclusions of our paper.

## 2. Bond-operators formalism

The bond-operator mean-field approach [15] is basically a strong coupling approximation in  $J$ . The spins between layers dominantly form singlets and the density of triplets is ‘low’ (this assumption will allow one to neglect triplet–triplet interaction). For two  $S = \frac{1}{2}$  spins, Sachdev and Bhatt [15] introduced four creation operators to represent the four states in Hilbert space. This basis can be created out of the vacuum by singlet  $|s\rangle$  and triplet  $|t_{\alpha}\rangle = t_{\alpha}^{\dagger}|0\rangle$  ( $\alpha = x, y, z$ ) operators. In terms of these triplet and singlet operators the localized and conduction electron spin operators are given by

$$\begin{aligned} S_{i,\alpha} &= \frac{1}{2} \left( s_i^{\dagger} t_{i,\alpha} + t_{i,\alpha}^{\dagger} s_i - i \epsilon_{\alpha\beta\gamma} t_{i,\beta}^{\dagger} t_{i,\gamma} \right), \\ \tau_{i,\alpha} &= \frac{1}{2} \left( -s_i^{\dagger} t_{i,\alpha} - t_{i,\alpha}^{\dagger} s_i - i \epsilon_{\alpha\beta\gamma} t_{i,\beta}^{\dagger} t_{i,\gamma} \right), \end{aligned} \quad (2)$$

where  $\alpha, \beta$  and  $\gamma$  take the values  $x, y, z$ , repeated indices are summed over, and  $\epsilon$  is the totally antisymmetric Levi–Civita tensor. The restriction that the physical states are either singlets or

triplets leads to the constraint  $s^\dagger s + \sum_\alpha t_\alpha^\dagger t_\alpha = 1$ . Moreover, the singlet and triplet operators at each site satisfy bosonic commutation relations  $[s, s^\dagger] = 1$ ,  $[t_\alpha, t_\beta^\dagger] = \delta_{\alpha,\beta}$ ,  $[s, t_\alpha^\dagger] = 0$ . Substituting the operator representation of spins defined in equation (2) into the original Hamiltonian equation (1) and considering the commutation relations, we obtain

$$H = H_0 + H_1 + H_2$$

where

$$\begin{aligned} H_0 &= \frac{J}{4} \sum_i \left( -3s_i^\dagger s_i + t_{i,x}^\dagger t_{i,x} + t_{i,y}^\dagger t_{i,y} + t_{i,z}^\dagger t_{i,z} \right) \\ &\quad + \sum_i \mu_i \left( s_i^\dagger s_i + t_{i,x}^\dagger t_{i,x} + t_{i,y}^\dagger t_{i,y} + t_{i,z}^\dagger t_{i,z} - 1 \right), \\ H_1 &= \frac{t_{\parallel}}{4} \sum_{i,\delta_1;\alpha} \left( s_i^\dagger s_{i+\delta_1}^\dagger t_{i,\alpha} t_{i+\delta_1,\alpha} + s_i^\dagger s_{i+\delta_1} t_{i,\alpha}^\dagger t_{i+\delta_1,\alpha}^\dagger \right) \\ &\quad - \frac{t_{\parallel}}{4} \sum_{i,\delta_1;\alpha} \left( t_{i,z}^\dagger t_{i+\delta_1,z}^\dagger t_{i,\alpha} t_{i+\delta_1,\alpha} - t_{i,z}^\dagger t_{i+\delta_1,z} t_{i,\alpha}^\dagger t_{i+\delta_1,\alpha}^\dagger + \text{h.c.} \right), \\ H_2 &= \frac{t_{\perp}}{4} \sum_{i,\delta_2;\alpha} \left( s_i^\dagger s_{i+\delta_2}^\dagger t_{i,\alpha} t_{i+\delta_2,\alpha} + s_i^\dagger s_{i+\delta_2} t_{i,\alpha}^\dagger t_{i+\delta_2,\alpha}^\dagger \right) \\ &\quad - \frac{t_{\perp}}{4} \sum_{i,\delta_2;\alpha} \left( t_{i,z}^\dagger t_{i+\delta_2,z}^\dagger t_{i,\alpha} t_{i+\delta_2,\alpha} - t_{i,z}^\dagger t_{i+\delta_2,z} t_{i,\alpha}^\dagger t_{i+\delta_2,\alpha}^\dagger + \text{h.c.} \right). \end{aligned} \quad (3)$$

Here  $\alpha = x, y$ .  $H_0$  represents the interaction between spins  $S$  and  $\tau$  in the site  $i$  and the constraint  $s^\dagger s + t_{i,x}^\dagger t_{i,x} + t_{i,y}^\dagger t_{i,y} + t_{i,z}^\dagger t_{i,z} = 1$  is implemented through the local chemical potentials  $\mu_i$ .  $H_1, H_2$ , are terms associated with the hopping  $t_{\parallel}$  and  $t_{\perp}$ , respectively. As argued before, we neglect triplet–triplet interactions [19].

### 3. Antiferromagnetic ordered phase

The Hamiltonian above, at half filling, can be simplified using a mean-field decoupling [20]. Relying on the nature of the strong coupling limit  $(t/J) \rightarrow 0$  we take  $\langle s_i^\dagger \rangle = \langle s_i \rangle = \bar{s}$ . Next, to describe the condensation of one local Kondo spin triplet  $t_{\mathbf{k},x}$  on the AF reciprocal vector  $Q = (\pi/a, \pi/a, \pi/a)$ , we introduce:  $t_{\mathbf{k},x} = \sqrt{N\bar{t}}\delta_{\mathbf{k},Q} + \eta_{\mathbf{k},x}$  corresponding to *fixing the orientation of the localized spins along the x direction*. The quantity  $\bar{t}$  is the mean value of the  $x$ -component spin triplet in the ground state and  $\eta_{\mathbf{k},x}$  represents the fluctuations. Finally the translation invariance of the problem implies that we may assume the local chemical potential as a global one.

Making approximations already used in the bond-operator formalism [16, 17] and after performing a Fourier transformation of the boson operators, we get

$$\begin{aligned} H_{mf} &= N \left( -\frac{3}{4} J \bar{s}^2 + \mu \bar{s}^2 - \mu \right) + \left( \frac{J}{4} + \mu \right) \sum_{\mathbf{k}} t_{\mathbf{k},z}^\dagger t_{\mathbf{k},z} \\ &\quad + \left( \frac{J}{4} + \mu - \frac{1}{2} \bar{s}^2 (t_{\parallel} Z_{\parallel} + t_{\perp} Z_{\perp}) \right) N \bar{t}^2 \\ &\quad + \sum_{\mathbf{k}} \left[ \Lambda_{\mathbf{k}} \eta_{\mathbf{k},x}^\dagger \eta_{\mathbf{k},x} + D_{\mathbf{k}} \left( \eta_{\mathbf{k},x}^\dagger \eta_{-\mathbf{k},x}^\dagger + \eta_{\mathbf{k},x} \eta_{-\mathbf{k},x} \right) \right] \\ &\quad + \sum_{\mathbf{k}} \left[ \Lambda_{\mathbf{k}} t_{\mathbf{k},y}^\dagger t_{\mathbf{k},y} + D_{\mathbf{k}} \left( t_{\mathbf{k},y}^\dagger t_{-\mathbf{k},y}^\dagger + t_{\mathbf{k},y} t_{-\mathbf{k},y} \right) \right], \end{aligned} \quad (4)$$

with  $\Lambda_{\mathbf{k}} = \omega_0 + 2D_{\mathbf{k}}$ ,  $\lambda(\mathbf{k})_{\parallel} = \cos k_x + \cos k_y$ ,  $\Delta_{\mathbf{k}} = \frac{1}{4} t_{\parallel} \bar{s}^2 \lambda(\mathbf{k})_{\parallel}$ ,  $\lambda(\mathbf{k})_{\perp} = \cos k_z$ ,  $\Delta'_{\mathbf{k}} = \frac{1}{4} t_{\perp} \bar{s}^2 \lambda(\mathbf{k})_{\perp}$ ,  $D_{\mathbf{k}} = \Delta_{\mathbf{k}} + \Delta'_{\mathbf{k}}$ ,  $N$  is the number of lattice sites,  $Z_{\parallel} = 4$  is the total

number of the nearest neighbors in planes and  $Z_{\perp} = 2$  is the number of the nearest neighbors between planes. The wavevectors  $k$  are taken in the first Brillouin zone and the lattice spacing was assumed to be unity. We have considered for simplicity a cubic lattice.

Now we obtain the free energy; for that, we shall employ the equation of motion method using the Green's functions and thus to obtain the thermal averages  $\langle H_{mf} \rangle = U$ . So the thermal averages of the singlet and triplet correlation functions are obtained from

$$\langle \langle \gamma_{\mathbf{k},\alpha}; \gamma_{\mathbf{k},\alpha}^{\dagger} \rangle \rangle_{\omega} = \frac{1}{2\pi} \frac{\omega + \Lambda_{\mathbf{k}}}{\omega^2 - \omega_{\mathbf{k}}^2}, \quad \langle \langle t_{\mathbf{k},z}; t_{\mathbf{k},z}^{\dagger} \rangle \rangle_{\omega} = \frac{1}{2\pi} \frac{1}{\omega - \omega_0}, \quad (5)$$

where  $\gamma = \eta, (t)$  for  $\alpha = x, (y)$ . The poles of the Green's functions determine the excitation energies of the system as  $\omega_0 = (J/4 + \mu)$ , which is the dispersionless spectrum of the longitudinal spin triplet states and  $\omega_{\mathbf{k}} = \pm \sqrt{\Lambda_{\mathbf{k}}^2 - (2D_{\mathbf{k}})^2}$  that correspond to the excitation spectrum of the transverse spin triplet states for both branches  $\omega_x = \omega_y$ . Then, we can stress that the contribution of the term  $k = Q$  for the free energy from the bosons  $t_{k,x}$  will depend only on the average value  $\bar{t}$  in the expression and not on the energy spectrum of the bosons. Consequently the Green's function for both  $\alpha = x$  and  $y$  is the same. Solving the coupled equations of motion obtained for the Green's function propagators we obtain

$$U = \langle \mathcal{H}_{mf} \rangle = \varepsilon_0 + \frac{\omega_0}{2} \sum_{\mathbf{k}} \left( \coth \frac{\beta \omega_0}{2} - 1 \right) + \sum_{\mathbf{k}} \omega_{\mathbf{k}} \left( \coth \frac{\beta \omega_{\mathbf{k}}}{2} - 1 \right), \quad (6)$$

where

$$\varepsilon_0 = N \left( -\frac{3}{4} J \bar{s}^2 + \mu \bar{s}^2 - \mu \right) + N \left( \frac{J}{4} + \mu - \frac{1}{2} \bar{s}^2 (t_{\parallel} Z_{\parallel} + t_{\perp} Z_{\perp}) \right) \bar{t}^2 + \sum_{\mathbf{k}} (\omega_{\mathbf{k}} - \omega_0), \quad (7)$$

is the ground state energy of the system,  $\beta = 1/k_B T$ ,  $\bar{s}$  and  $\bar{t}$  being the singlet and triplet order parameters, respectively.

Considering the above equation (6) and that the entropy of free bosons is  $S = k_B \sum_{\mathbf{k}} [(n(\omega_{\mathbf{k}}) + 1) \ln(n(\omega_{\mathbf{k}}) + 1) - n(\omega_{\mathbf{k}}) \ln(n(\omega_{\mathbf{k}}))]$ , the free energy  $F = U - TS$  is trivially obtained as

$$F = \varepsilon_0 - \frac{2}{\beta} \sum_{\mathbf{k}} \ln[1 + n(\omega_{\mathbf{k}})] - \frac{N}{\beta} \ln[1 + n(\omega_0)], \quad (8)$$

where  $n(\omega) = \frac{1}{2} (\coth \frac{\beta \omega}{2} - 1)$  is the occupation factor for bosons. Since the parameter  $\bar{s}$  is always nonzero [19, 18] and  $\bar{t} \neq 0$  in the antiferromagnetic phase, we minimize the ground state energy with respect to  $\bar{t}$  to find  $\mu = t_{\parallel} \bar{s}^2 / y - J/4$ , and consequently  $\omega_{\mathbf{k}} = \frac{1}{y} t_{\parallel} \bar{s}^2 \sqrt{1 + y(\lambda(\mathbf{k}_{\parallel}) + \xi \lambda(\mathbf{k}_{\perp}))}$  where  $\xi = t_{\perp} / t_{\parallel}$  is the real spatial anisotropy ratio between the hopping along different directions and  $y = 1/(2 + \xi)$ . Then, we can calculate the other parameters  $\bar{s}^2 = \bar{s}^2(T)$  and  $\bar{t}^2 = \bar{t}^2(T)$  minimizing the free energy equation (8). Using  $(\partial \varepsilon / \partial \mu, \partial \varepsilon / \partial \bar{s}) = (0, 0)$ , we can easily get the following saddle-point equations:

$$\begin{aligned} \bar{s}^2 &= 1 + \frac{J}{t_{\parallel}} \frac{y}{2} - \frac{1}{2N} \sum_{\mathbf{k}} \sqrt{1 + y(\lambda(\mathbf{k}_{\parallel}) + \xi \lambda(\mathbf{k}_{\perp}))} \coth \frac{\beta \omega_{\mathbf{k}}}{2} - \varsigma, \\ \bar{t}^2 &= 1 - \frac{J}{t_{\parallel}} \frac{y}{2} - \frac{1}{2N} \sum_{\mathbf{k}} \frac{1}{\sqrt{1 + y(\lambda(\mathbf{k}_{\parallel}) + \xi \lambda(\mathbf{k}_{\perp}))}} \coth \frac{\beta \omega_{\mathbf{k}}}{2} - \varsigma, \end{aligned} \quad (9)$$

where  $\varsigma = \frac{1}{4} (\coth \frac{\beta \omega_0}{2} - 1)$ . Generally the equations for  $\bar{s}$  and  $\bar{t}$  in equation (9) should be solved and at  $\xi = 0$ , ( $\xi = 1$ ) the results of [20] for 2d (3d) are recovered. For  $J/t_{\parallel} > (J/t_{\parallel})_c$ , triplet excitations remain gapped and at  $J/t_{\parallel} < (J/t_{\parallel})_c$  the ground state has both condensation of singlets and triplets at the antiferromagnetic wavevector  $Q = (\pi, \pi, \pi)$ . Then, the QCP at  $T = 0$ ,  $(J/t)_{\perp}$  separates an antiferromagnetic long-range ordered phase from a gapped spin

liquid phase. For finite temperatures, the condensation of singlets  $s$  occurs at a temperature scale which, to a first approximation, tracks the exchange  $J$ . The energy scale below which the triplet excitations condense is given by the Néel temperature ( $T_N$ ) which is calculated in the next section near the AF magnetic instability.

#### 4. Néel temperature in the AKNM

The Néel line giving the finite temperature instability of the antiferromagnetic phase for  $J/t_{\parallel} < (J/t_{\parallel})_c$  is obtained as the line in the  $T$  versus  $(J/t_{\parallel})$  plane at which  $\bar{t}$  vanishes ( $\bar{t} = 0$ ). Thereby from equation (9) we have

$$\frac{J}{t_{\parallel}} = \frac{2}{y} \left( 1 - \frac{1}{2N} \sum_{\mathbf{k}} \frac{1}{\sqrt{1 + y(\lambda(\mathbf{k})_{\parallel} + \xi\lambda(\mathbf{k})_{\perp})}} \coth \frac{\beta\omega_{\mathbf{k}}}{2} + \varsigma \right). \quad (10)$$

This expression defines the boundary of the AF state. Consequently the QCP is obtained making  $T = 0$  in equation (10), then we get

$$\left( \frac{J}{t_{\parallel}} \right)_c = \frac{2}{y} \left( 1 - \frac{1}{2N} \sum_{\mathbf{k}} \frac{1}{\sqrt{1 + y(\lambda(\mathbf{k})_{\parallel} + \xi\lambda(\mathbf{k})_{\perp})}} \right), \quad (11)$$

where  $y = 1/(2 + \xi)$  as defined before. Because  $g = |(J/t_{\parallel})_c - (J/t_{\parallel})|$  measures the distance to the QCP we finally obtain

$$|g| = \frac{1}{yN} \sum_{\mathbf{k}} \frac{1}{\sqrt{1 + y(\lambda(\mathbf{k})_{\parallel} + \xi\lambda(\mathbf{k})_{\perp})}} \left( \coth \frac{\beta\omega_{\mathbf{k}}}{2} - 1 \right) + \frac{2\varsigma}{y}. \quad (12)$$

##### 4.1. Numerical results at $T = 0$

In order to find the AF boundary at  $T = 0$  we are going to calculate as the QCP varies from 2d to 3d, i.e. as we turn on  $\xi$ . Our numerical task consists in evaluating, at various  $\xi$ , the quantum critical point given by equation (11). For this purpose we first consider the isotropic cases, i.e.  $\xi = 1$  (3d) with  $t_{\parallel} = t_{\perp} = t$ , and  $\xi = 0$  (2d) where  $t_{\parallel} = t$  and  $t_{\perp} = 0$ . Thereby we easily obtain  $J/t \approx 1.4409$  ( $J/t \approx 2.6611$ ) in 2d (3d) in agreement with previous works in the KNM [19] as well as KLM [18]. In figure 1 we have plotted the coupling strength  $(J/t_{\parallel})_c$  versus the anisotropy at  $1 - \xi$  for different  $\xi \in [0, 1]$ . The inset shows the log-log plot of  $g$  versus  $\xi$  close to  $d = 2$  ( $\xi \in [0, 0.1]$ ,  $g = |(J/t_{\parallel})_c - (J/t_{\parallel})_{c2d}|$  and  $(J/t_{\parallel})_{c2d} \approx 1.4409$ ). The line fit yields  $g \propto \xi^{1.8}$ .

In summary, in this section we have established the essential expression, equation (12), for finding the Néel temperature as a function of  $g$  and  $\xi$  as well as the QCP dependence on the anisotropy  $\xi$ . In the next section we are going to use the calculations above to investigate analytically if there is thermodynamic phase transition when inter-plane hopping  $t_{\perp}$  is turned on.

#### 5. Analytical results for finite temperature

In this section we are going to calculate analytically the Néel critical line for both the q2d ( $\xi \ll 1$ ) and q3d ( $\xi \approx 1$ ) AKNM. The case  $\xi \gg 1$  that corresponds to  $d = 1$  will be shown only to give continuity to our analysis. All the calculations will be done considering two essential approximations: (i) the system is close to a magnetic instability; (ii) the temperature region where the Néel line will be found will be lower than the Kondo temperature ( $T_K$ ).

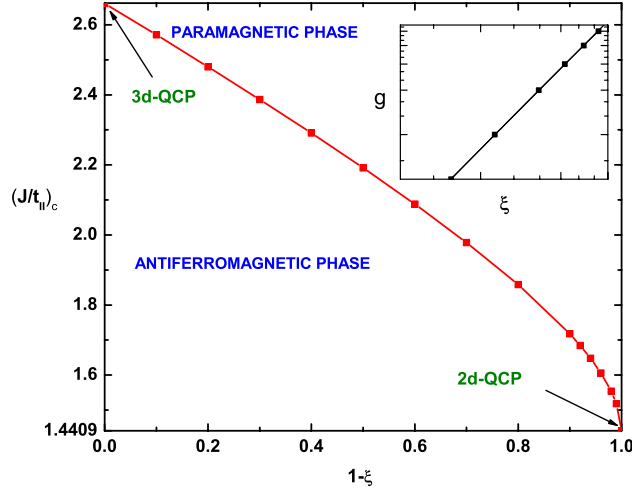


**Figure 1.** Zero temperature phase diagram showing the line of quantum phase transitions  $(J/t_{\parallel})_c$  as a function of the anisotropy parameter  $1 - \xi$ . Also shown is the AF border  $(J/t_{\parallel})_c$  at 2d (2d-QCP  $\approx 1.4409$ ) and 3d (3d-QCP  $\approx 2.6611$ ). The points were obtained by solving equation (11). The inset shows the log–log plot of  $g$  versus  $\xi$  close to  $d = 2$  ( $\xi \in [0, 0.1]$ ),  $g = |(J/t_{\parallel})_c - (J/t_{\parallel})_{c2d}|$  and  $(J/t_{\parallel})_{c2d} \approx 1.4409$ . The line fit yields  $g \propto \xi^{1.8}$ .

We will start expanding  $k$  close to the wavevector  $\mathbf{Q} = (\pi, \pi, \pi)$  associated with the antiferromagnetic instability, so we get

$$\begin{aligned}\lambda(\mathbf{k})_{\parallel} &= -2 + \frac{k_{\parallel}^2}{2} + O(k_{\parallel}^4), \\ \lambda(\mathbf{k})_{\perp} &= -1 + \frac{k_z^2}{2} + O(k_z^4).\end{aligned}\quad (13)$$

This yields the spectrum of transverse spin triplet excitations as

$$\omega_{\mathbf{k}} = \omega_0 \sqrt{1 + y(\lambda(\mathbf{k})_{\parallel} + \xi \lambda(\mathbf{k})_{\perp})} \approx \omega_0 \sqrt{\frac{y}{2}(k_{\parallel}^2 + \xi k_z^2)}, \quad (14)$$

where  $\omega_0$  is the  $z$ -polarized dispersionless branch of excitations. Replacing equation (14) in equation (12), and considering that for temperatures  $k_B T \ll \omega_0$ ,  $\zeta$  goes to zero faster than the first term of equation (12), we obtain

$$|g| \frac{y}{2} = \frac{1}{\pi^2} \int_0^{\pi} \int_0^{\pi} \frac{k_{\parallel} dk_{\parallel} dk_z}{\sqrt{\frac{y}{2}(k_{\parallel}^2 + \xi k_z^2)}} \left( \coth \frac{\beta \omega_{\mathbf{k}}}{2} - 1 \right). \quad (15)$$

For  $\xi = 0$  the integral above diverges, excluding long-range order at finite temperatures in two dimensions in accord with the Mermin–Wagner theorem [21]. On the other hand, when  $\xi = 1$ , the in-plane interaction equals the inter-plane coupling ( $t_{\perp} = t_{\parallel}$ ) and we have a pure 3d KNM with  $T_N \propto \sqrt{|g|}$  as found in a previous work [20].

### 5.1. The case $\xi \ll 1$

We now demonstrate analytically the appearance of a finite Néel line temperature when a small hopping  $t_{\perp}$  between planes is turned on. Making a change of variables in equation (15) we obtain

$$|g| = \frac{1}{y^2 \pi^2 \alpha} \int_0^{\pi} \left( \int_a^b (\coth u - 1) du \right) dk_z, \quad (16)$$

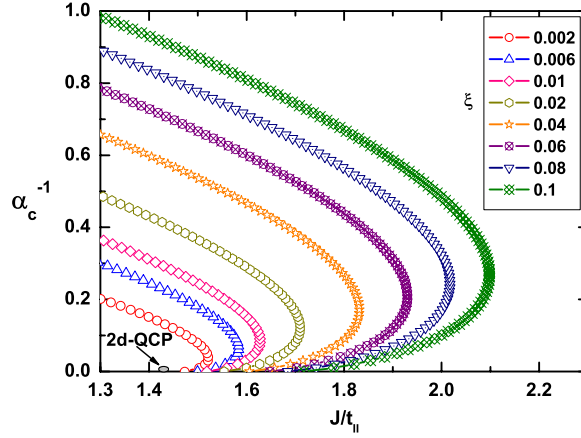


**Figure 2.** Phase diagram between the temperature as  $\alpha_c^{-1}$  and  $J/t_{||}$  for nonzero  $\xi$ . We observe that Néel order arises for an arbitrarily weak inter-plane hopping  $t_{\perp}$  and it increases as  $\xi$  increases. 2d-QCP shows the zero temperature quantum critical point in 2d ( $\xi = 0$ ). The interesting feature of this phase diagram is the reentrant behavior for  $0.002 < \xi < 0.1$ . As temperature is lowered, the system passes from a disordered paramagnetic phase (with no spontaneous symmetry breaking), to the antiferromagnetic phase, and back to the disordered phase as the temperature is lowered further.

where  $u = 2\alpha\sqrt{\frac{y}{2}(k_{||}^2 + \xi k_z^2)}$ ,  $b = 2\alpha\sqrt{y(\pi^2 + \xi k_z^2)}/2$ ,  $a = 2\alpha\sqrt{\xi y/2}k_z$  and  $\alpha = \omega_0/4k_B T$ . While each of the Kondo systems has its own energy scale Kondo temperature  $T_K$  below which the thermodynamic and transport properties are governed by the QCP [22], relevant perturbation which is normally present in real systems introduces another energy scale  $T_x$  where crossover to another regime occurs (for instance, the *coherence temperature* proposed by Continentino and collaborators [23]). In our case we argue that the Néel temperature region can be observed only when  $T_x/T_K \ll 1$ . In other words, the Néel region can be observed only for  $\alpha \gg 1$  (since  $\omega_0$  tracks  $J \sim T_K$ ). Thereby, solving equation (16) considering the latter and  $\xi \ll 1$  we get

$$|g|_{\xi \ll 1} = 2\sqrt{\xi} + \frac{4}{\pi\alpha} \left[ 1 - \ln(2\pi\sqrt{\xi}\alpha) \right] + O(\xi), \quad (17)$$

where we took  $y \approx (1 - \frac{\xi}{2})/2$  and the second term in the right-hand side takes into account the thermal fluctuations. Equation (17) gives us the Néel line as a function of the distance to QCP  $g$  for a small but finite anisotropy  $\xi$  and temperatures  $k_B T \ll \omega_0$ , where as said before  $\omega_0$  tracks  $T_K$ . We observe in equation (17) that  $|g|$  diverges for  $\xi = 0$ , then in two dimensions there is no AF ordering above zero temperature. As soon as the dimension of the AKNM is greater than two, there is a nonzero-temperature phase transition.

In figure 2 we show the phase diagram  $\alpha_c^{-1} = 4k_B T_N/\omega_0$  as a function of  $J/t_{||}$  for different value of  $\xi$  between  $[2 \times 10^{-3}, 10^{-1}]$ .  $\alpha_c^{-1}$  is defined as the critical line where Néel order appears. We observe a reentrance phenomenon that will be discussed in the following subsection. Close to the isotropic 3d-QCP the system does not display this phenomenon. At this point we can construct the phase diagram  $\alpha_c^{-1}$  versus  $J/t_{||}$  versus  $1 - \xi$  for  $\xi \ll 1$  considering our analytical and numerical calculations. This is shown in figure 3, where the boundary line at  $T = 0$  has been calculated using equation (11) and the Néel lines using equation (17).

In summary, in this subsection we have obtained analytically the expression for the Néel line close to the QCP in q2d and we have shown that in fact this line exists for  $\xi \ll 1$  and



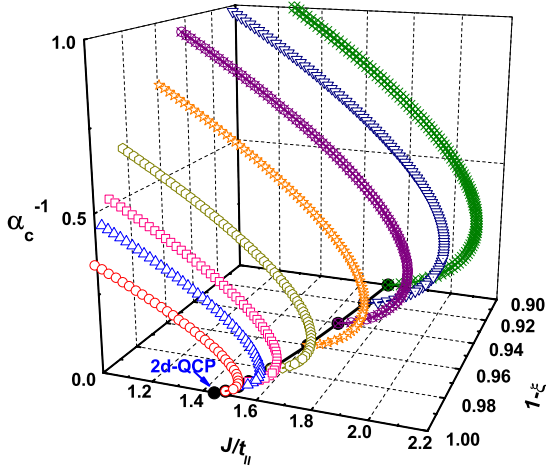


**Figure 3.** Three-dimensional phase diagram showing the critical Néel temperature as  $\alpha_c^{-1}$  versus  $J/t_{||}$  and  $1 - \xi$ . The Néel temperature increases rapidly as  $\xi$  increases for small  $\xi$ . This shows that very weak inter-plane coupling  $t_{\perp}$  is enough to destroy the 2d character of the second-order transition. As long as the dimension of the AKNM is greater than two, there is a nonzero-temperature phase transition.

temperatures much smaller than the exchange interaction energy  $J$ . We now are going to analyze the causes of the reentrance observed in figure 2.

*5.1.1. Reentrance in the quasi-two-dimensional AKNM.* Reentrant behavior has posed challenges to microscopic theoretical physics in a variety of condensed matter systems [24–30]. This phenomenon is characterized by the reappearance of a less ordered phase, following a more ordered one, as the temperature is lowered. It appears that the reentrance phenomenon also occurs, as we report in this paper, in the phase diagram of a quasi-two dimensional AKNM, at least as indicated from our bond-operator mean-field theory calculation. Basically the reentrant phenomenon can be produced by the increase of entropy due to disorder or due to the presence of additional degrees of freedom. In terms of our level scheme this can be explained as due to the competition between singlet and triplet type ground states. There is a combined free energy gain from the energy condensation of the singlets and the entropy associated with the triplet states at low but finite temperatures for  $\xi \ll 1$ . In our case dimensional effects also play a role in the reentrance phenomenon since at 2d there is no finite temperature transition. At the highest temperatures uncorrelated fluctuations determine the thermodynamics. The system is then in the disordered paramagnetic phase but with a AF bias due to the exchange interaction ratio  $J/t_{||}$  (as distinguished from spontaneous symmetry breaking). As temperature is lowered to around  $T_N$ , energy and entropy are both important, and the correlated fluctuations affect the dominance of either phase significantly. The system enters the AF phase. At the lowest temperatures, energy but not entropy is important and the ground-state energy of either phase determines the dominance. To our knowledge this effect has not been observed experimentally. Hence, we hope that our results will stimulate further experiments in this field.

## 5.2. The case $\xi \approx 1$

We have calculated in the preceding section the q2d antiferromagnetic state for the AKNM, which allowed us to study the effect of inter-plane hopping  $t_{\perp}$  on the emergence of the Néel critical line. We now calculate it for the q3d AKNM. For our purposes, it is sufficient to consider

$$\xi = 1 - \epsilon, \quad (18)$$

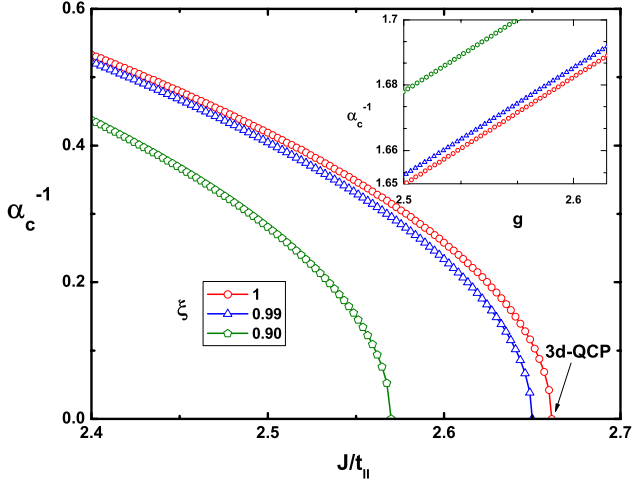


**Figure 4.** Phase diagram between the temperature for  $\alpha_c^{-1}$  versus  $J/t_{\parallel}$  for  $\xi \approx 1$ . We observe that the Néel line is only renormalized when the inter-plane hopping  $t_{\perp} \sim t_{\parallel}$ . The inset shows the log-log plot of  $\alpha_c^{-1}$  versus  $g$ . The Néel line scales like  $T_N \sim g^{\psi}$  with  $\psi \approx 0.5$  close to the 3d-QCP.

where  $\epsilon$  is a dimensionless parameter that controls the dimensional crossover in this case. Close to 3d the anisotropy ratio will be  $\xi \approx 1$ , hence  $\epsilon \ll 1$ . Thereby, working in analogy with the preceding section, using equations (15) and (18) we obtain

$$|g|_{\xi \approx 1} = \frac{\sqrt{6}}{8} \frac{1}{\alpha^2} (3 - \epsilon + O(\epsilon^2)). \quad (19)$$

The equation above shows that the Néel line of the q3d AKNM ( $\xi \approx 1$ ) is only renormalized by the anisotropy ratio  $\epsilon$ . Thus, for  $\epsilon = 0$ , the in-plane interaction equals the inter-plane hopping ( $t_{\perp} = t_{\parallel}$ ) and we recover the exact value as obtained in a previous work for the isotropic KNM [20]. Figure 4 displays the Néel line close to 3d-QCP for  $\xi = 0.9, 0.99, 1$ . The inset shows the log-log plot of  $\alpha_c^{-1}$  versus  $J/t_{\parallel}$ . The Néel line scales like  $T_N \sim g^{\psi}$  with  $\psi \approx 0.5$ . We conclude that, in the q3d AKNM the Néel line exists and goes to zero as  $T_N \propto \sqrt{|g|}$ .

### 5.3. The case $\xi \gg 1$

In order to give continuity to our analysis we might also consider the case  $\xi \rightarrow \infty$ . Since now the coupling between planes is large ( $t_{\perp} \gg t_{\parallel}$ ), we may treat it using the same scheme as before where the ratio  $\xi = t_{\perp}/t_{\parallel}$  is taken as a huge parameter. Then we can see easily that considering  $\xi \rightarrow \infty$  in equation (15) gives us zero, ensuring that there is no long-range order at finite temperatures in 1d KNM [21].

In summary, in this subsection we have shown that an analytical treatment leads to an exactly solvable and comprehensible relation between the dimension and Néel line, which can be used to gain insight into the role of the dimensionality in SCES.

## 6. Conclusions

In this paper we considered the AKNM at zero and low temperatures. Our main motivation for undertaking the present study has been to determine whether there is a well-defined crossover region when the anisotropy ratio  $\xi = t_{\perp}/t_{\parallel}$  varies from zero (2d) to one (3d). We have succeeded in finding that the Néel line already exists since turning on the inter-plane hopping  $t_{\perp}$ , although in general, geometric anisotropy is an extremely fragile mechanism for decoupling spin planes and will always be overcome by quantum and thermal fluctuations. Our work was also motivated by heavy fermion systems. These are much more complex systems than

the insulating Kondo systems at half-filling presented here. Nevertheless, we believe that our mechanism for the formation of a q2d Néel line by means of a real spatial anisotropy survives in the case of more complicated SCES. It emphasizes the need to consider the effects of dimensionality in a more realistic generalization of the widely accepted views that follow from Doniach's Kondo necklace model. We are led to conclude that inter-plane coupling is essential to keep 3d AF ordering at finite temperatures. Therefore there are AF phase transitions for  $\xi > 0$  at the Néel temperature  $T_N > 0$ .

Although the transport properties related to the kinetic energy of conduction electrons are not quantitatively represented in the Hamiltonian (1), the most essential features of Kondo lattices, i.e. the competition between a long-range ordered state and a disordered state is clearly retained in the model. The qualitative features regarding the stability of the AF phase are well displayed in the model and it allows a simple physical interpretation of the phase diagram in anisotropic Kondo lattices. It will be left to a further work to compare our theoretical results obtained for the AKNM with both experimental data and different levels of approximation in order to clarify to what extent the estimates of  $\xi$  from measured quantities depend on the theoretical tools used.

### Acknowledgments

The authors would like to thank the Brazilian agencies FAPERJ and CNPq for financial support.

### References

- [1] Reyes D and Continentino M A 2007 *Physica B* at press
- [2] Sachdev S 2000 *Science* **288** 475–80
- [3] Stockert O, von Lohneysen H, Rosch H, Pyka N and Loewenhaupt M 1998 *Phys. Rev. Lett.* **80** 5627–30
- [4] Si Q, Rabello S, Ingersent K and Smith J L 2001 *Nature* **413** 804–8
- [5] Mathur N D *et al* 1998 *Nature* **394** 39–43
- [6] Senthil T, Vishwanath A, Balents L, Sachdev S and Fisher M P A 2004 *Science* **303** 1490–4
- [7] Millis A J 1993 *Phys. Rev. B* **48** 7183–96
- [8] Batista C D and Nussinov Z 2005 *Phys. Rev. B* **72** 045137
- [9] Xu C and Moore J E 2005 *Phys. Rev. B* **72** 064455
- [10] Continentino M A 1993 *Phys. Rev. B* **47** 11587
- [11] Moriya T and Takimoto T 1995 *J. Phys. Soc. Japan* **64** 960
- [12] Hertz J A 1976 *Phys. Rev. B* **14** 1165
- [13] Si Q, Rabello R, Ingersent K and Smith J 2001 *Nature* **413** 804
- [14] Doniach S 1977 *Physica B* **91** 231
- [15] Sachdev S and Bhatt R N 1990 *Phys. Rev. B* **41** 9323
- [16] Gopalan S, Rice T M and Sigrist M 1994 *Phys. Rev. B* **49** 8901
- [17] Normand B and Rice T M 1996 *Phys. Rev. B* **54** 7180
- [18] Jurecka C and Brenig W 2001 *Phys. Rev. B* **64** 092406
- [19] Zhang G-M, Gu Q and Yu L 2000 *Phys. Rev. B* **62** 69
- [20] Reyes D and Continentino M A 2007 *Phys. Rev. B* **76** 075114
- [21] Mermin N D and Wagner H 1966 *Phys. Rev. Lett.* **17** 1133
- [22] Continentino M A 2001 *Scaling in Many-Body Systems* (Singapore: World Scientific)
- [23] Continentino M A, Japiasu G and Troper A 1989 *Phys. Rev. B* **39** 9734
- [24] Fertig J G and Maple M B 1974 *Solid State Commun.* **15** 453
- [25] Simanek E 1981 *Phys. Rev. B* **23** 5762
- [26] Cladis P E 1975 *Phys. Rev. Lett.* **35** 48
- [27] Tinh N H, Hardouin F and Destrade C 1982 *J. Physique* **43** 1127
- [28] Indekeu O J and Berker A N 1986 *Phys. Rev. A* **33** 1158
- [29] Manheimer A M, Bhagat S M and Chem H S 1982 *Phys. Rev. B* **26** 456
- [30] Vasconcelos dos Santos R J, Sa Barreto F C and Coutinho S 1990 *J. Phys. A: Math. Gen.* **23** 2563